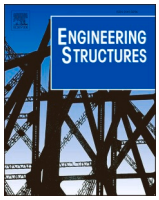
Engineering Structures 319 (2024) 118824



Contents lists available at ScienceDirect

Engineering Structures

journal homepage: www.elsevier.com/locate/engstruct





Novel strengthening method of signal tower using prestressed CFRP plates: Concept and behavior

Xu Liang [a,b], Yunhao Wang [c], Peng Feng [d], Lili Hu [a,b,*]

[a] State Key Laboratory of Ocean Engineering, School of Ocean and Civil Engineering, Shanghai Jiao Tong University, Shanghai 200240, China
[b] Shanghai Key Laboratory for Digital Maintenance of Buildings and Infrastructures, Shanghai Jiao Tong University, Shanghai 200240, China
[c] College of Smart Energy, Shanghai Jiao Tong University, Shanghai 200240, China
[d] Key Laboratory of Civil Engineering Safety and Durability of China Education Ministry, Department of Civil Engineering, Tsinghua University, Beijing 100084, China

ARTICLE INFO

Keywords:
Signal tower
Prestressed CFRP
Strengthening
Wind load
Design procedure

ABSTRACT

A novel prestressed carbon fiber reinforced polymer (CFRP) plate strengthening method for signal towers was proposed. The proposed strengthening system incorporates a circumferential anchorage system, a support system, a column system, and CFRP plates. These elements synergistically interact with the tower, forming a self-balancing system. This integrated system can provide exceptional flexural capacity and reduce the lateral displacement of the tower under wind load. To validate this novel method, a series of four static load tests were conducted. The results showed that the initial stiffness of the strengthened tower with CFRP plate prestresses of 0, 200, and 400 MPa increased by 71.0 %, 113.8 %, and 113.8 % compared with the unstrengthened tower, respectively. Moreover, the CFRP plate slacking occurred later for the strengthened tower with higher CFRP plate prestress, and the stiffness of the tower after the CFRP plate slacking kept increasing as CFRP plate prestress increases. The results indicate that the prestressed CFRP plate strengthening method effectively improved the behavior of the tower under wind load. Moreover, the finite element method (FEM) was utilized to analyze the influence of the ratio of the circumferential anchorage system height to tower height, the ratio of the support system height to tower height, the ratio of the column height to tower height, the ratio of steel support length to tower diameter, the elastic modulus of the CFRP plate and CFRP plate prestress on the strengthening effect. Finally, a strengthening procedure was proposed according to FEM results and sensitivity analysis. The analysis findings can serve as a guide for designing the strengthening system.

1. Introduction

The rapid advancement of information technology and the development of intelligent cities have created an urgent need to upgrade mobile base stations and install new 5 G signal equipment on existing signal towers. The additional weight will impose a load on the existing towers and potentially affect their stability. Additionally, there has been a notable increase in the frequency of weather and climate disasters in recent years [1], exposing signal towers to potential damage from severe weather conditions like storms and hurricanes. Furthermore, the continuous exposure of towers to environmental factors, including vibrations, can contribute to fatigue and subsequent structural degradation. Consequently, it is imperative to strengthen the towers to not only withstand the additional equipment load but also ensure stability under wind load and counteract the effects of fatigue.

There have been several classical strengthening methods proposed by researchers and commercial companies for signal towers. The strengthening principle is to enhance the flexural stiffness of towers. A traditional approach to strengthening tower structures involved constructing truss elements and prestressed steel cables around the tower [2,3], while these methods were commonly applied to towers situated in spacious environments. Additionally, various alternative approaches to strengthen tower structures are summarized in Table 1. Steel tubes, steel plates, steel bars, cement, and concrete were utilized in strengthening towers [4–12]. Welding was utilized in the strengthening methods (a) and (b) to connect the steel components to the tower. For the strengthening method (c), a cylinder shell mold was used and filled with cement or glass fiber-reinforced concrete. Welding was avoided in the

* Correspondence to: Shanghai Key Laboratory for Digital Maintenance of Buildings and Infrastructures, State Key Laboratory of Ocean Engineering, School of Naval Architecture, Ocean and Civil Engineering, Shanghai Jiao Tong University, Shanghai 200240, China.
E-mail address: lilihu@sjtu.edu.cn (L. Hu).

https://doi.org/10.1016/j.engstruct.2024.118824
Received 30 March 2024; Received in revised form 23 July 2024; Accepted 15 August 2024
Available online 30 August 2024
0141-0296/© 2024 Elsevier Ltd. All rights are reserved, including those for text and data mining, AI training, and similar technologies.

Table 1
Summary of strengthening methods using steel, cement, and concrete.

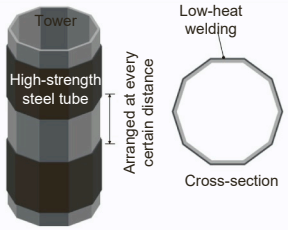
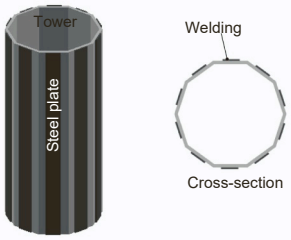
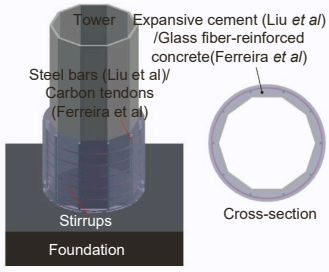
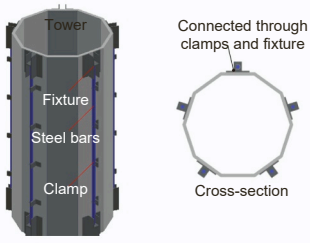
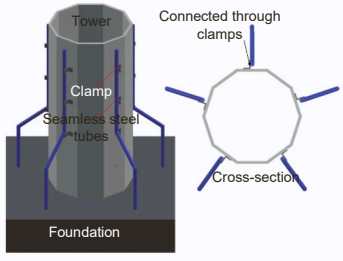
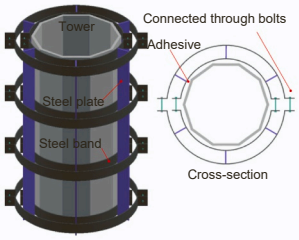
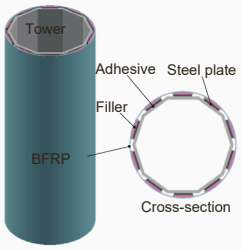
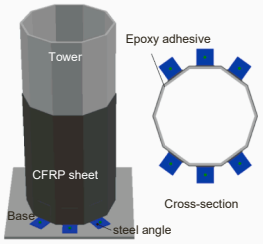
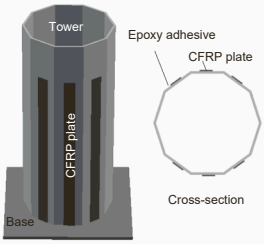
Researcher /Company	Strengthening method	Strengthening diagram
Morisson *et al* [4]	(a) High-strength steel tube strengthening method: prefabricating high-strength steel tubes fitting the outer cross-section of the tower to encase the tower by low-heat welding.	
Hu *et al* [5]/ Hutter Trankina Engineering [6]	(b) Steel plates strengthening method: laying out the steel plates symmetrically around the longitudinal axis of the tower.	
Liu *et al* [7] / Ferreria *et al* [8]	(c) Expansive cement/Glass-fiber reinforced concrete strengthening method: using cylinder shell mold and filled with expansive cement/ glass-fiber reinforced concrete to increase the section inertial moment.	
Westower Communication [9]	(d) High-strength threaded bars strengthening method: high-strength threaded bars installed in parallel with the tower shaft, serving as the structural backbone.	
Westower Communication [10]	(e) Cable tower strengthening method: the length of the seamless steel tubes was extensible according to requirements and steel tubes can be prestressed.	
Fort Worth Tower Company [11]	(f) Steel plates and steel bands strengthening method: longitudinal steel plates were bolted at the ends to steel bands and then steel bands are bonded to the shaft surface using epoxy adhesives.	

Table 2
Summary of strengthening methods using FRP materials.

Researcher /Company	Strengthening method	Strengthening diagram Strengthening effect
Guo *et al* [14]	(g) the steel plates were directly bonded to the original tower surface and BFRP was wrapped around the entire structure to integrate it with the original tower.	
Lanier *et al* [15]	(h) using CFRP and recommended specific connections for CFRP and tower.	
AeroSolution company [16]	(i) CFRP plates bonded parallel to tower shafts to increase the flexural behavior.	

strengthening methods (d) and (e), and fixtures and clamps were utilized to connect the steel components to the tower. For the strengthening method (f), adhesives were utilized to bond the steel bands to the shaft surface of the tower, and steel plates were fixed by steel bands.

Fiber-reinforced polymer (FRP) has shown excellent behaviors in strengthening structures due to fatigue resistance, corrosion resistance, low weight, and high-strength properties [12–17]. FRP strengthening method is cost-effective and easy to install. The installation of FRP on the tower can be accomplished within a relatively short time without welding. The serviceability and durability of strengthened towers can be enhanced due to the excellent properties of FRP. The strengthening methods using FRP materials are summarized in Table 2. Steel plates

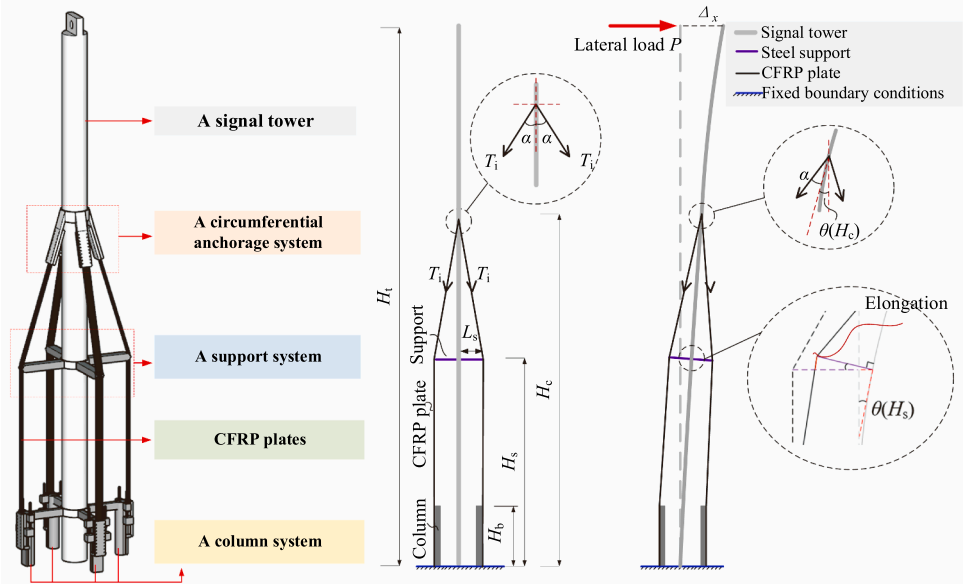
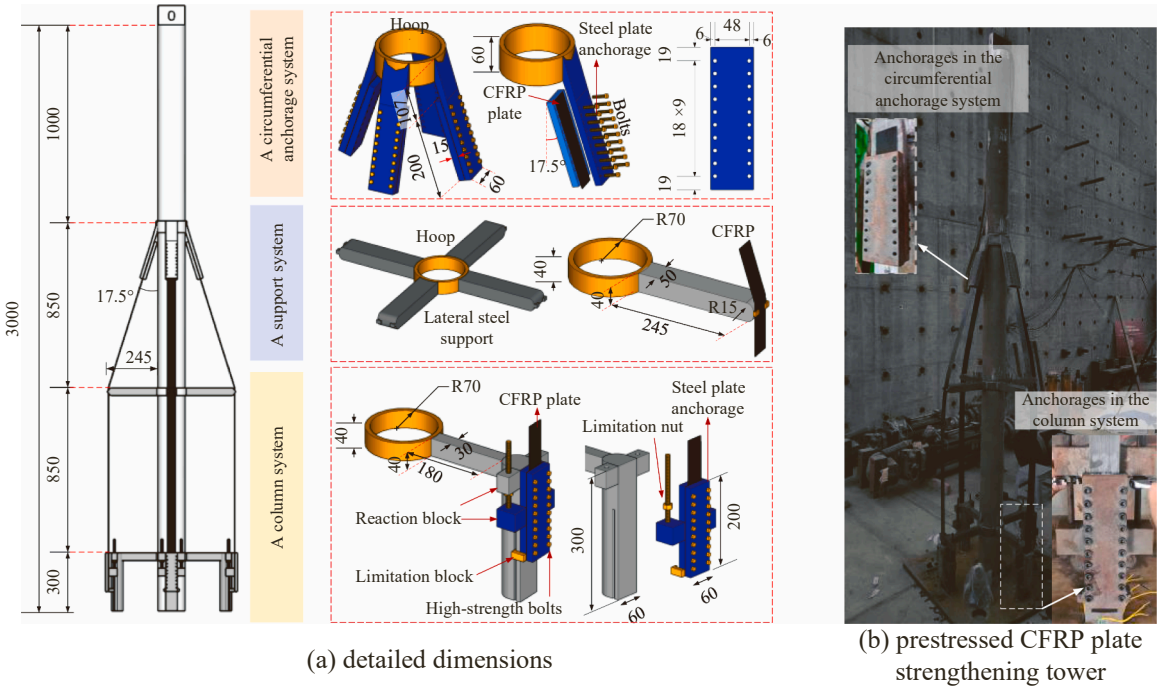


Fig. 1. Prestressed CFRP plate strengthening signal tower system.



(a) detailed dimensions

(b) prestressed CFRP plate strengthening tower

Fig. 2. Details of prestressed CFRP plate strengthening signal tower (unit: mm).

were bonded to the tower in strengthening method (g) [18] to increase the area of cross-section, and basalt fiber-reinforced polymer (BFRP) material provided corrosion protection to the towers. Strengthening methods (h) [19] and (i) [20] involved the utilization of epoxy adhesive to connect carbon fiber-reinforced polymer (CFRP) plates and sheets to the tower. Furthermore, some researchers have conducted analysis to explore the application of shape memory alloy in strengthening steel structures, which provided a promising strengthening method for signal towers [21,22].

In practical scenarios, signal towers endure varying wind loads and their device needs updating, thus it is important for strengthened towers to have the ability to adjust to the increasing loads. Additionally, when implementing strengthening methods, it is vital to avoid interfering with the pedals on the tower used for maintenance and consider any space limitations that may be present around the tower. Therefore, a novel prestressed CFRP plate strengthening method for signal towers has been proposed. CFRP plate prestress can be increased to enhance the strengthening effect according to the increased load and CFRP plates can be installed without affecting the entire structure. Moreover, the method requires minimal land area. In this paper, the concept, and the mechanism of the prestressed CFRP plates strengthening method are first introduced. Then, experimental tests are conducted on the scaled tower with and without prestressed CFRP plate strengthening under wind load. Finally, the numerical model established in ABAQUS [23] is verified by the experiments and the effect of relevant parameters of the strengthening system is studied on the behavior of the strengthened tower. Finally, the recommendation of a strengthening design procedure is proposed to guide the design of the strengthening system based on parametric sensitivity analysis.

2. Concept

2.1. Strengthening method

A signal tower strengthened by prestressed CFRP plates consists of a circumferential anchorage system, a support system, a column system, and CFRP plates (Fig. 1). Two ends of CFRP plates are anchored by the circumferential anchorage system and the column system, and the middle part of CFRP plates is supported by the support system. Specifically, the circumferential anchorage system is composed of a connecting hoop and four steel plate anchorages; the support system is composed of a connecting hoop and four lateral steel supports; the column system is composed of a connecting hoop, steel supports, columns, and steel plate anchorages. Lateral steel supports and steel plate anchorages are welded to the corresponding hoop, respectively; four vertical columns are welded to a lateral support system and fixed on the ground. CFRP plates were prestressed by moving the anchorages downward in the column system.

2.2. Mechanism

A prestressed CFRP plate strengthening signal tower is a self-balancing system. Initially, CFRP plates at opposite directions are prestressed and have the same tensile force T_i. The angle between the CFRP plate at both sides and the tower is both α. Before wind load is applied to the signal tower, the signal tower is compressed by the vertical force caused by prestressed CFRP plates, which is disadvantageous to the behavior of the tower. After applying wind load on the tower, the tensile force at the left and right sides increases. Then the horizontal forces at the circumferential system height and the support system height caused by different CFRP plate prestresses are generated, which has an opposite and same direction with the wind load, respectively. Some assumptions are made to obtain the displacement at the top of the tower: (1) wind load is equivalent to the concentrated load P at the top of the tower; (2) CFRP plates at both sides are under tension; (3) the effect of vertical force is ignored; (4) the materials are in the linear elastic state. According to the bending moment equilibrium equations and displacement boundary conditions, the displacement at the loading point Δx is calculated by Eq. (1), and the deflection angle θ at the circumferential system height and the support system height can be obtained by Eqs. (2) and (3), respectively.

$$\Delta x = x_{P,P} - x_{P,C} + x_{P,S} = \frac{2PH_t^3 - P_cH_c^2(3H_t - H_c) + P_sH_s^2(3H_t - H_s)}{6E_sI_s} \quad (1)$$

$$\theta(H_c) = \frac{PH_c(2H_t - H_c)}{2E_sI_s} \tag{2}$$

$$\theta(H_s) = \frac{PH_s(2H_t - H_s)}{2E_sI_s} \tag{3}$$

where $x_{P,P}$, $x_{P,C}$, and $x_{P,S}$ refer to the displacement at the loading point caused by the force at the loading point, the circumferential system height, and the support system height, respectively. H_t, H_c, and H_s are the tower height, the circumferential system height, and the support system height, respectively. E_s and I_s are the elastic modulus and inertia moment of a steel tower, respectively. P_c and P_s are the resultant forces in the horizontal direction at the circumferential system height and the support system height, respectively.

According to geometrical conditions, the elongation of CFRP plate ΔL is calculated by Eq. (4).

$$\Delta L = \sqrt{L_s^2 + L_s^2 - 2 \times L_s \times L_s \times \cos\left(\theta(H_s)\right)} = L_s\sqrt{2(1 - \cos(\theta(H_s)))} \tag{4}$$

where L_s is the support length.

According to physical conditions, the increase in CFRP plate tensile force ΔT can be calculated by Eq. (5).

$$\Delta T = E_pA_p\Delta L/L_c \tag{5}$$

where E_p and A_p are elastic modulus and cross-section area of CFRP plate, respectively; L_c is the total CFRP plate length before deformation and can be calculated by Eq. (6). Thus, Δx can be expressed using Eq. (7).

$$L_c = H_s - H_b + \sqrt{(H_c - H_s)^2 + L_s^2} \tag{6}$$

$$\begin{aligned}\Delta x &= x_{P,P} - x_{P,C} + x_{P,S} \\ &= \frac{2PH_t^3 - \left(\left(T_i + E_pA_p\dfrac{L_s\sqrt{2\left(1 - \cos\dfrac{PH_s(2H_t - H_s)}{2E_sI_s}\right)}}{H_s - H_b + \sqrt{(H_c - H_s)^2 + L_s^2}}\right)\sin\left(\dfrac{PH_c(2H_t - H_c)}{2E_sI_s} + \alpha\right)\right.}{6E_sI_s} \\ &\quad \frac{\left.\left(T_i - E_pA_p\dfrac{L_s\sqrt{2\left(1 - \cos\dfrac{PH_s(2H_t - H_s)}{2E_sI_s}\right)}}{H_s - H_b + \sqrt{(H_c - H_s)^2 + L_s^2}}\right)\sin\left(\alpha - \dfrac{PH_c(2H_t - H_c)}{2E_sI_s}\right)\right)H_c^2\left(3H_t - H_c\right)}{6E_sI_s} \\ &\quad + \frac{2E_pA_p\dfrac{L_s\sqrt{2\left(1 - \cos\dfrac{PH_s(2H_t - H_s)}{2E_sI_s}\right)}}{H_s - H_b + \sqrt{(H_c - H_s)^2 + L_s^2}}\sin\alpha\cos\dfrac{PH_s(2H_t - H_s)}{2E_sI_s}H_s^2\left(3H_t - H_s\right)}{6E_sI_s}\end{aligned} \tag{7}$$

The reduced displacement caused by the strengthening method is influenced by the initial angle α between CFRP plates and the tower, the ratio of the circumferential anchorage system height to tower height H_c/H_t, the ratio of the support system height to tower height H_s/H_t, the ratio of the column height to tower height H_b/H_t, the elastic modulus of CFRP (E_p) and CFRP plate prestress (T_i/A_p). The effect of these parameters will be analyzed in Section 4.3.

2.3. Advantages

The prestressed CFRP plate strengthening method has the following advantages: (1) due to the system generating forces that act in the opposite direction to the deformation, the strengthening effect is significant; (2) The strengthening systems require few materials and have a high level of prefabrication, resulting in high installment efficiency and contributing to overall cost-effectiveness; (3) the installation of the CFRP plates and columns requires minimal land area; (4) CFRP plates are corrosion resistant and have minimal prestress loss, resulting in significantly reduced maintenance costs in the long term; (5) the prestress level of CFRP plates can be adjusted by the anchorages in the column system, allowing for strengthening modifications based on variable load conditions; (6) CFRP plate has a low coefficient of thermal expansion (CTE), ensuring structural stability and high safety even under extreme temperature conditions; (7) all strengthening parts are connected to the signal tower by bolts without welding, and the strengthening process does not affect the functionality of the structure and avoid interfering with pedals.

3. Experiment

3.1. Specimens and test program

The maximum horizontal displacement of a towering signal tower located in Fujian Province exceeds the standard requirement under wind load [24]. Based on this project, the tower is scaled and the prestressed CFRP plate strengthening method is utilized to assess the behavior of the strengthened tower under wind load. The height of the tower is scaled at a ratio of 1:10, while the thickness of the tower is scaled at the same ratio because of the small thickness. Thus, the cross-section of the tower is scaled with a ratio of 1: 100 based on the inertia moment. The designed scale tower is a steel tube with an outer diameter and thickness of 140 mm and 10 mm, respectively. The elastic modulus and yield strength of steel are 206 GPa and 499 MPa according to standard tensile tests, respectively [25]. The thickness and width of the CFRP plate are 1.2 and 40 mm, respectively. The elastic modulus and yield strength of steel and CFRP plate are 200 GPa and 2800 MPa, respectively. The detailed dimensions and position of other parts are shown in Fig. 2.

For the circumferential anchorage system, CFRP plates are compressed by steel plate anchorages using twenty high-strength bolts with a diameter of 6 mm, and surfaces between CFRP plates and anchorages

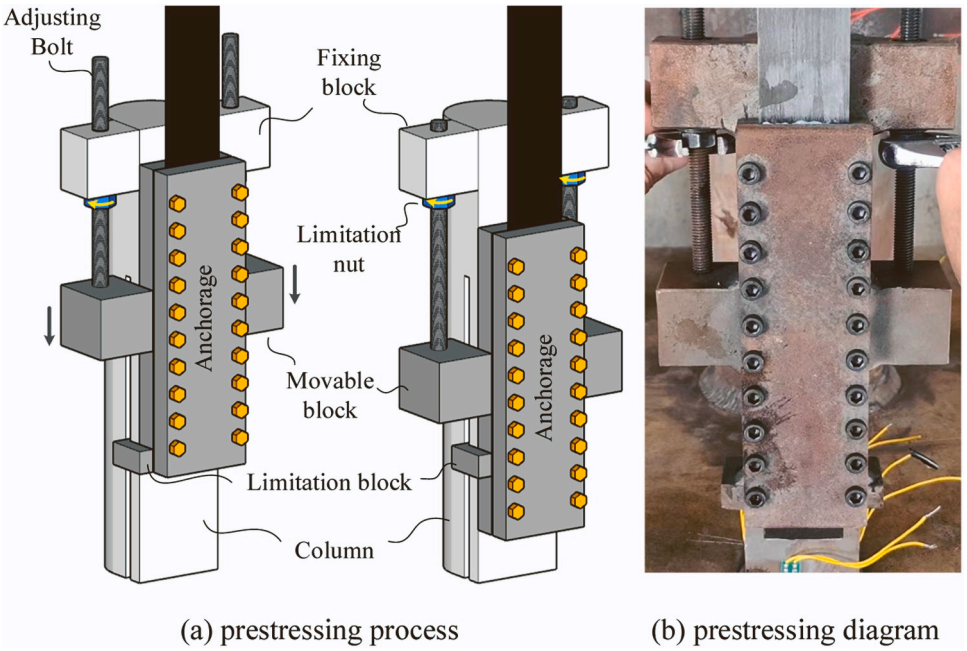


Fig. 3. Prestressing process and diagram.

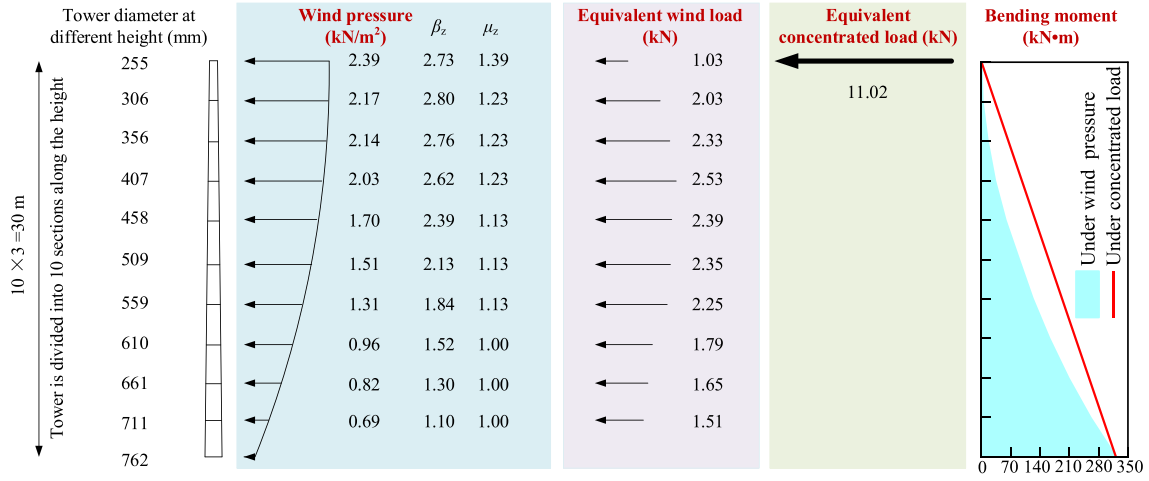


Fig. 4. Wind pressure and equivalent wind load.

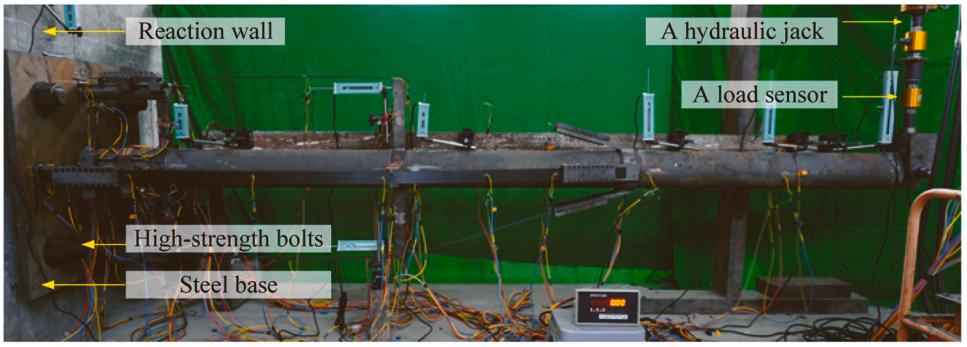


Fig. 5. Loading on site.

are sandblasted to improve friction. Then the acrylate adhesive is utilized to ensure a firm connection. The anchorage is composed of two steel plates with thickness and width of 15 mm and 60 mm, respectively. The anchorage length is set as 200 mm based on the studies [16,17] and the number of bolts is determined based on the anchorage length and the sufficient pressure for clamping CFRP plates. Detailed distances between holes on the steel plate anchorage are shown in Fig. 2. For the support system, the design of hoop thickness and hoop height considers the weld

Table 3
Specimen design.

Specimen	With/without CFRP plates	CFRP plate prestress (MPa)	Load (kN)	Stiffness before the CFRP plate slacks (MPa)	Stiffness after the CFRP plate slacks (MPa)
U	Without	–	5	155.6	–
PS−0	With	0	10	266.1	–
PS−200		200	10	332.7	276.9
PS−400		400	19 (load until failure)	332.7	247.6

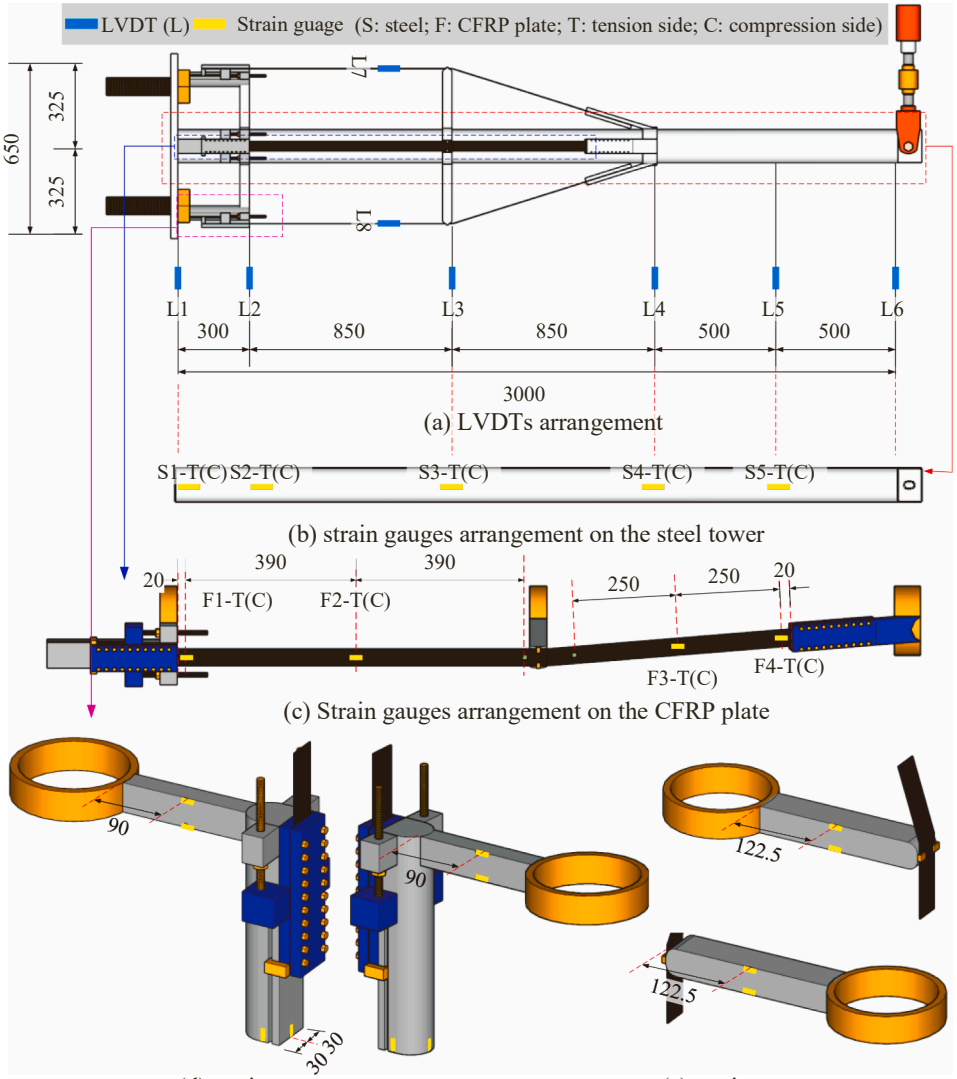


Fig. 6. Displacement and strain measurement (unit: mm).

size to ensure a stable welding connection and the cross-section dimensions of the lateral support are determined to prevent its buckling when subjected to axial compressive loading from the CFRP plates. The end of steel supports is chamfered to ensure uniform stress distribution, and surfaces between the steel supports and CFRP plates are covered with oil. Moreover, the end of steel supports is equipped with a restrictor to prevent CFRP plates from detaching from the support system. For the column system, the columns are equipped with limitation blocks and sliding rails, which match with the moveable blocks and the sliding blocks to ensure anchorages slide along the vertical direction during the prestressing procedure. The CFRP plates are compressed by anchorages using twenty high-strength bolts with a diameter of 6 mm. The distances between holes on steel plate anchorages in the column system are the same as those in the circumferential anchorage system. The surfaces between the steel plates and CFRP plates are sandblasted to improve the friction and the acrylate adhesive is utilized to ensure the firm connection. After CFRP plates are firmly connected to the anchorages, the adjusting blots are moved downward by simultaneously twisting the limitation nuts, and adjusting bolts will press against movable blocks, then steel plate anchorages will move downward with the blocks. Thus, CFRP plates can be prestressed (Fig. 3).

For the signal tower located in Fujian province, the wind pressure at different heights of the signal tower can be obtained by Eq. (7) according to GB 50009–2019 [26].

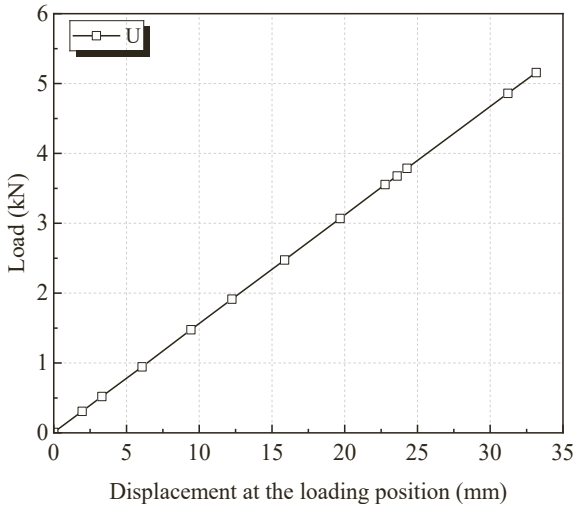


Fig. 7. Load-displacement curve of specimen U.

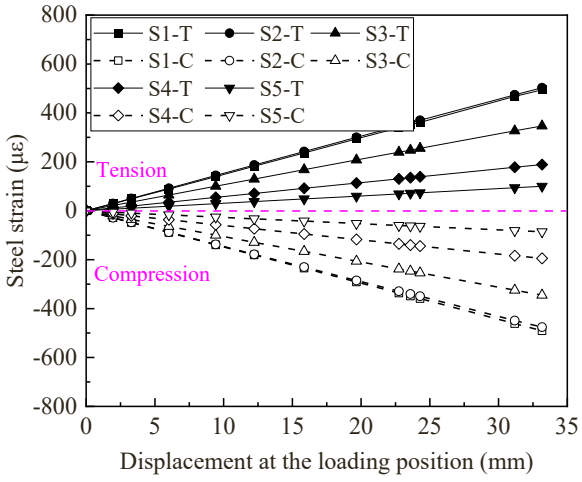


Fig. 8. Steel strain-displacement curves of specimen U.

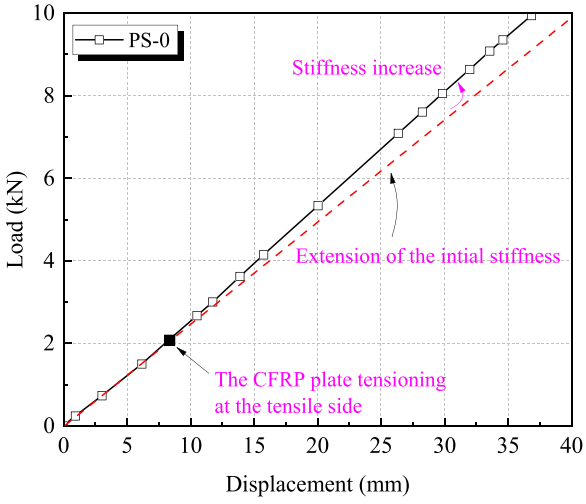


Fig. 9. Load-displacement curve of specimen PS-0.

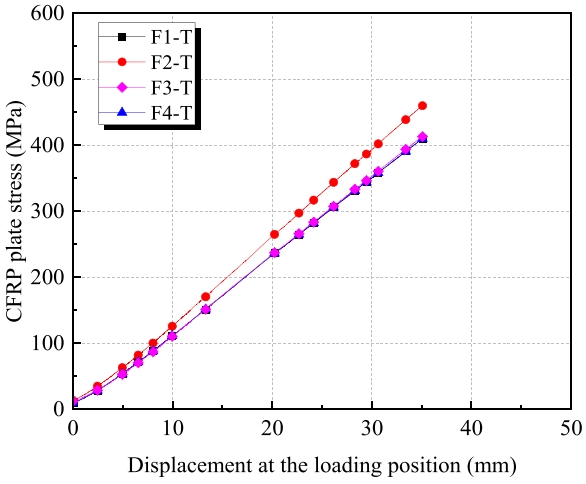


Fig. 10. CFRP plate stress-displacement curve of specimen PS-0.

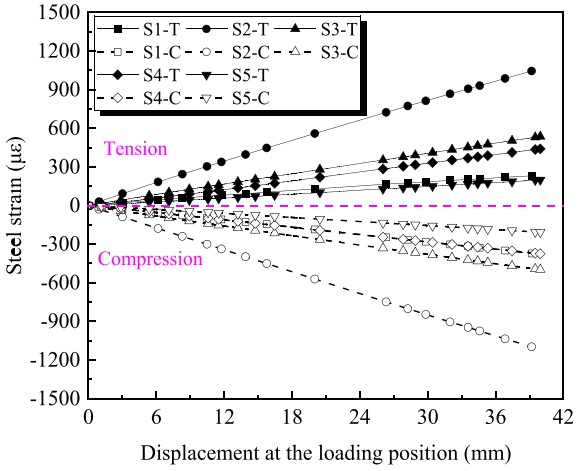


Fig. 11. Steel strain-displacement curve of specimen PS-0.

$$w_k = \beta_z \mu_s \mu_z w_0 \tag{7}$$

where w_k is the wind load standard value (kN/m^2); β_z is the wind vibration coefficient at height z; μ_s and μ_z are the wind load shape factor (taken as 0.9 for the cylinder shape) and wind pressure height variation coefficient, respectively; w_0 is basic wind load (kN/m^2). In the case of the signal tower located in Fujian province, the ground roughness is classified as category B, referring to the environment with sparse houses.

To calculate the wind pressure, the signal tower is averagely divided into ten segments. The tower height, tower diameter, wind pressure, wind vibration coefficient, and wind pressure height variation coefficient are shown in Fig. 4. The equivalent wind load can be calculated by Eq. (8).

$$F_{w,n} = w_{k,n} \times (A_n + A_{n+1})/2 \tag{8}$$

where $F_{w,n}$ is the equivalent wind load at the height of the n segment; $w_{k,n}$ is the wind pressure at the height of the n segment; A_n and A_{n+1} are the cross-section area bearing wind load at the n^{th} and $(n+1)^{th}$ segment.

The wind pressure is calculated according to GB50009–2019 [26]; based on it, the equivalent wind load at different heights is obtained; further, an equivalent concentrated load at the top of the tower is obtained, as shown in Fig. 4. The bending moment of the signal tower

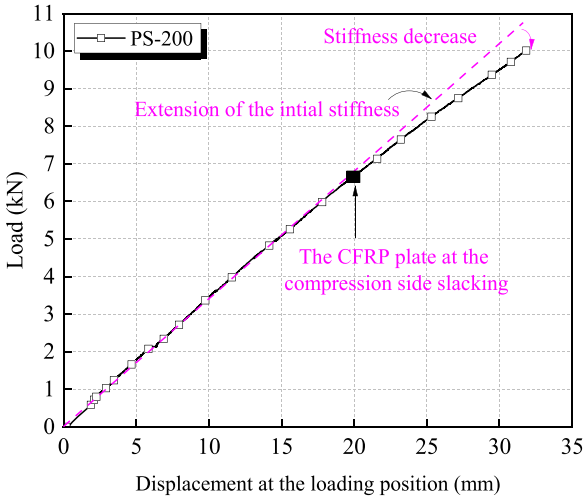


Fig. 12. Load-displacement curve of specimen PS-200.

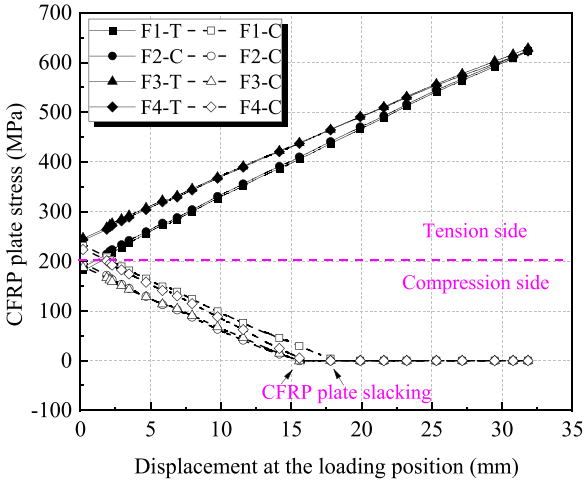


Fig. 13. CFRP plate stress-displacement curve of specimen PS-200.

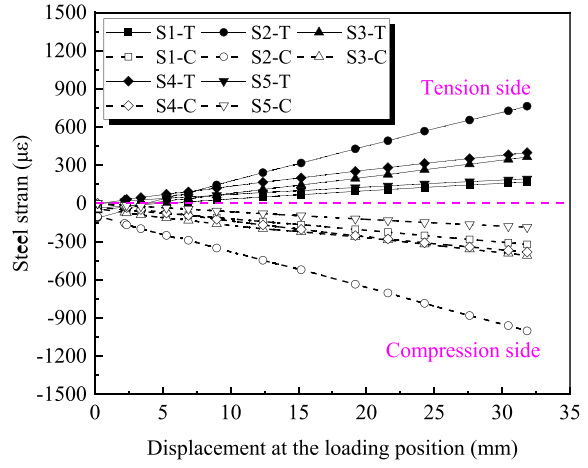


Fig. 14. Steel strain-displacement curve of specimen PS-200.

under the uniform wind pressure is not larger than that under the concentrated load, indicating that the concentrated load can result in more adverse stress distribution on the signal tower. Additionally, applying a concentrated load can be more convenient compared to

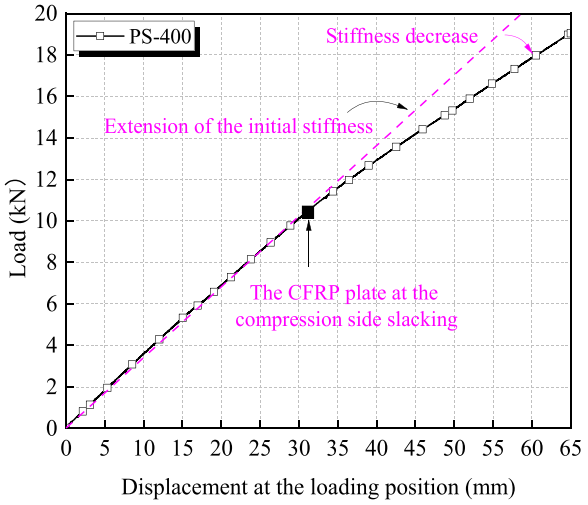


Fig. 15. Load-displacement curve of specimen PS-400.

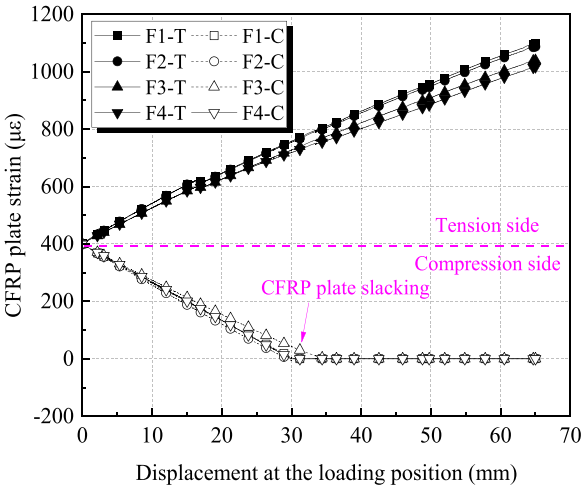


Fig. 16. CFRP plate strain-displacement curve of specimen PS-400.

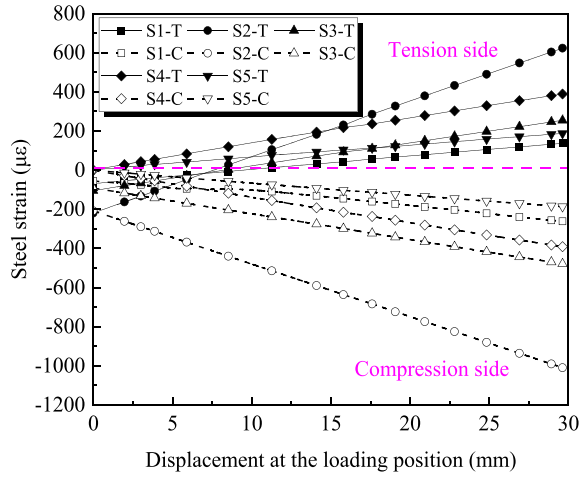


Fig. 17. Steel strain-displacement curve of specimen PS-400.

uniform wind pressure for experimental studies. Therefore, the concentrated load is applied to the specimens in the experiments.

For the test program, the steel tube and columns were welded to a

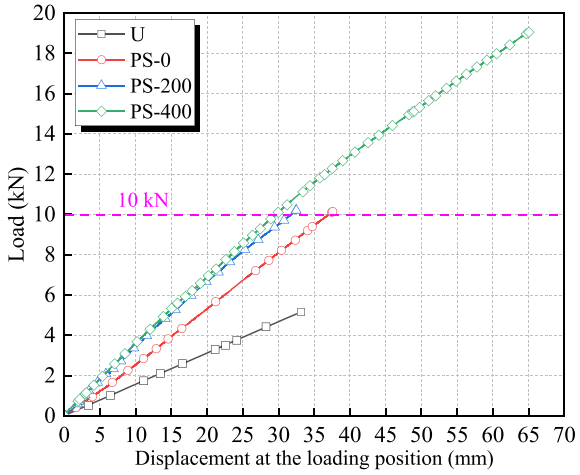


Fig. 18. Load-displacement curve of four specimens.

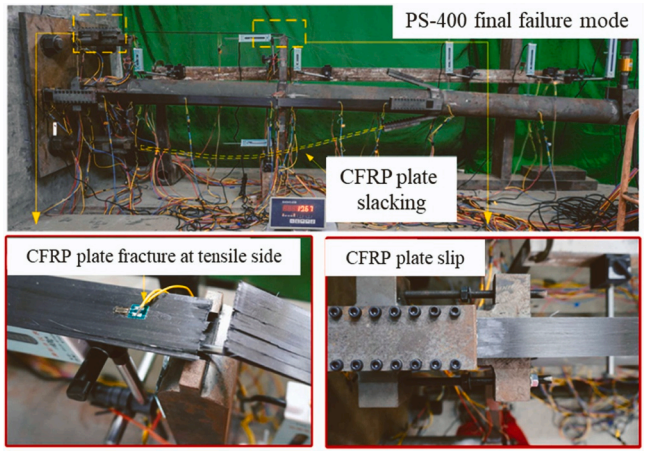


Fig. 19. Final failure mode of specimen PS-400.

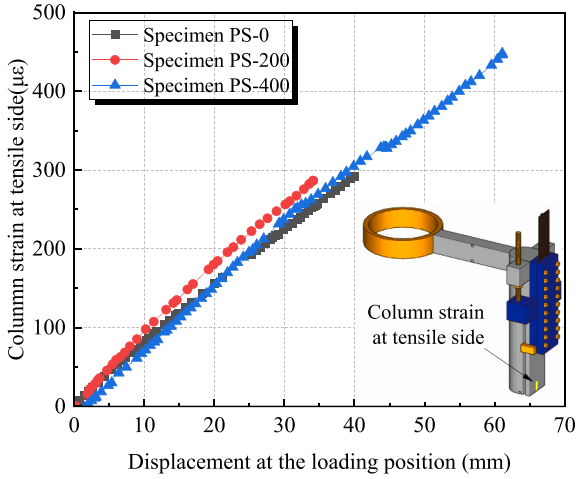


Fig. 20. Column strain-displacement curves of strengthened towers.

steel base plate and then installed to the reaction wall to simulate the rigid boundary condition. The load was applied at the cantilever end by a hydraulic jack and the load was obtained by a load sensor (Fig. 5). Before the tower was strengthened with prestressed CFRP plates, the steel tube was applied a load of 5 kN and the specimen was named U; for

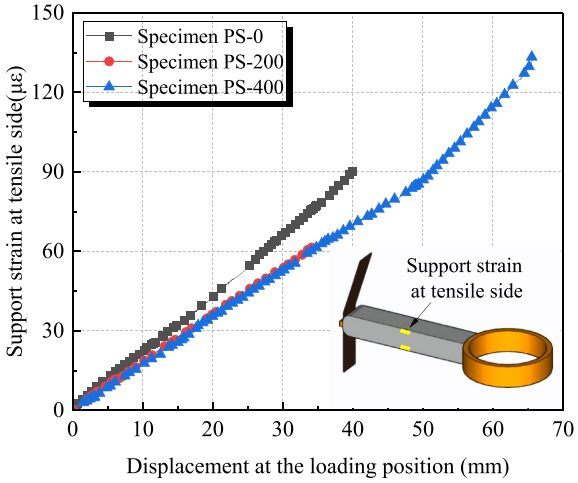


Fig. 21. Support strain-displacement curves of strengthened towers.

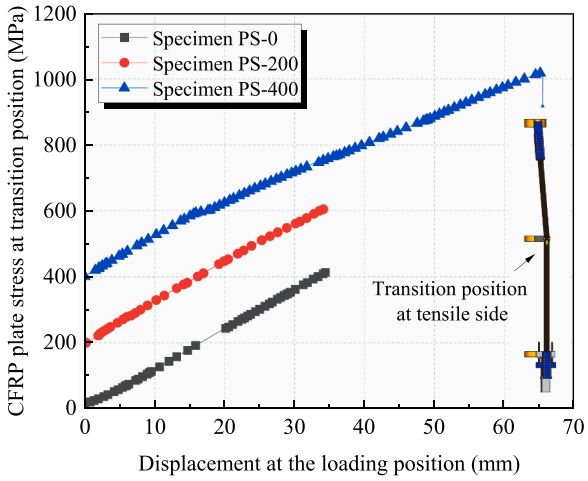


Fig. 22. CFRP plate stress-displacement curves of strengthened towers.

CFRP strengthening signal towers, CFRP plate prestress of specimens PS-0 and PS-200 was set as 0 and 200 MPa, respectively, and the load was set as 10 kN; CFRP plate prestress of specimen PS-400 was set as 400 MPa and the load was applied at the end of steel tube until the specimen failed. More details can be found in Table 3.

The linear variable differential transformers (LVDTs) were arranged to measure the vertical and horizontal displacements of specimens with and without CFRP plate strengthening. Strain gauges were arranged on the surface of four CFRP plates to monitor CFRP plate stress variation. Moreover, strain gauges were arranged at the surface of supports and columns. SX and FX represented steel and CFRP plate strain at different positions shown in Fig. 6, respectively; T and C referred to the tensile and compressive sides of the steel tube, respectively. The detailed arrangement of LVDTs and strain gauges can be found in Fig. 6.

3.2. Results

For specimen U, the relationship between load and displacement is shown in Fig. 7. Load-displacement curve showed a linear relationship and when the load was 5 kN, the maximum steel strain was smaller than 600 $\mu\varepsilon$ (Fig. 8), indicating that the steel tube was in the linear elastic stage. The absolute value of tension and compression strain was almost the same at different displacements, indicating that the neutral axis passed through the center of the annular section.

For specimen PS-0, the load-displacement curve is shown in Fig. 9,

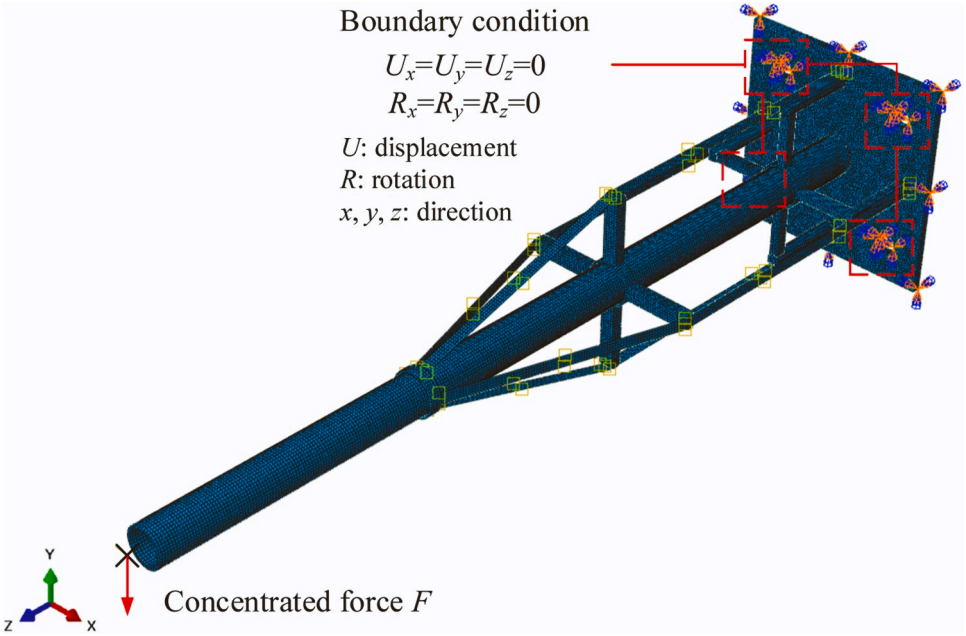


Fig. 23. Meshing and boundary condition.

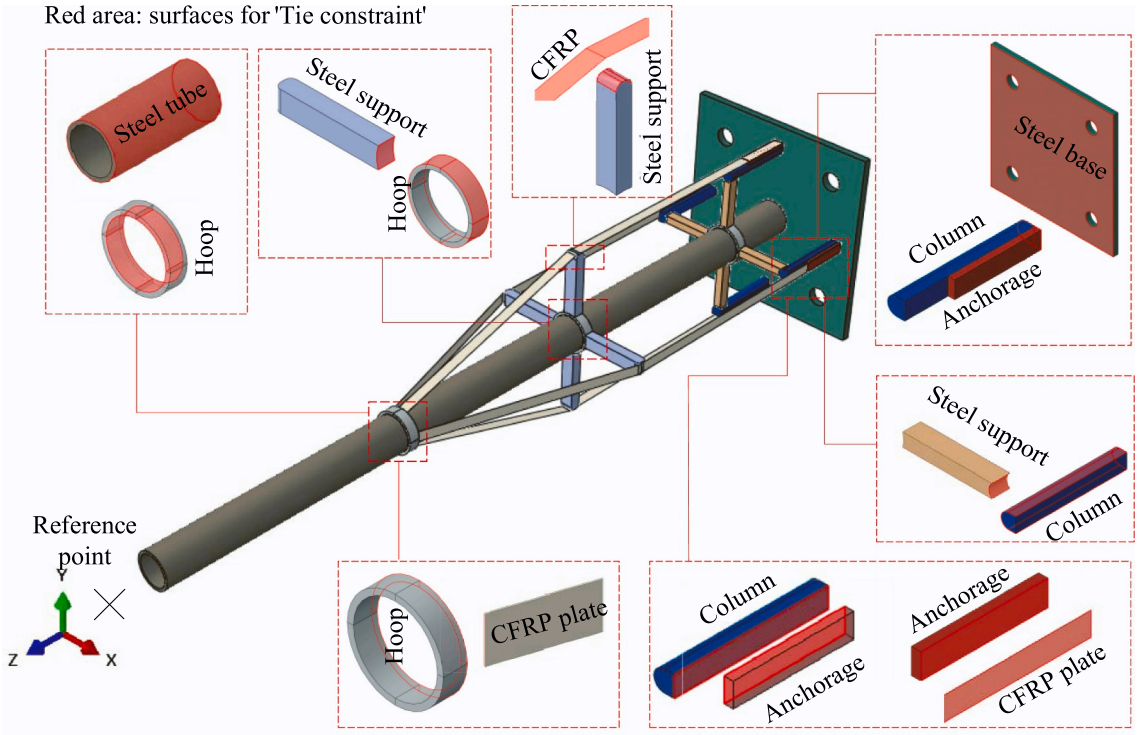


Fig. 24. Interaction definition between different parts.

and stress/strain-displacement curves are shown in Figs. 10 and 11. CFRP plate strain increased linearly with displacement. The absolute value of steel strain at the tension side was smaller than that at the compression side at the same displacement. The stiffness of the system started to increase and this was because CFRP plates on the tension side and the steel tube formed a combined cross-section and were jointly stressed. The results showed that CFRP plates could increase the stiffness of the system when they were in a tension state.

For specimen PS-200, the load-displacement curve is shown in Fig. 12, and stress/strain-displacement curves are shown in Figs. 13 and 14. As the concentrated load increased, CFRP plate strain at the tension and compression sides increased and decreased, respectively. When the concentrated load was smaller than 6.5 kN, CFRP plates at both sides was prestressed. CFRP plates at both sides and the steel tube formed a combined cross-section, which was jointly stressed, and the stiffness of the system was almost the same with the increase in displacement. After the concentrated load is larger than 6.5 kN, CFRP plate strain at the compression side remained almost constant and the CFRP plate slacking occurred, resulting in a decrease in the stiffness of the system. The results showed that the CFRP plate slacking could lead to a stiffness decrease.

For specimen PS-400, the load-displacement curve is shown in

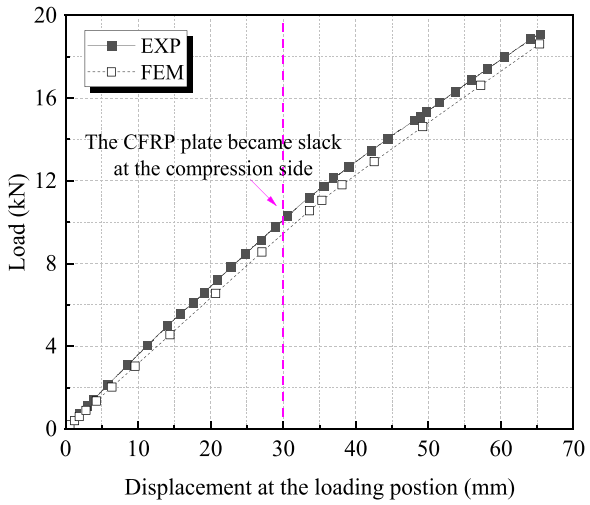


Fig. 25. Comparison of load-displacement curve of specimen PS-400 between EXP and FEM.

Fig. 15, and stress/strain-displacement curves are shown in Figs. 16 and 17. Steel and CFRP plate strain variations of specimen PS-400 had a similar tendency to those of specimen PS-200. The notable distinction was that the concentrated load of 11 kN caused the CFRP plate to slack at the compression side. Moreover, compared with specimens PS-200 and PS-400, the displacement corresponding to CFRP plate slacking was larger, indicating that the system exhibited better behavior with higher CFRP plate prestress.

3.3. Discussion

3.3.1. Comparison of specimens

The relationship between load and displacement of four specimens is shown in Fig. 18. For specimens U, PS-0, and PS-200, when the load was smaller than 10 kN, the load-displacement curve showed approximately linear relationships and the maximum steel strain was smaller than the yield strain. Compared with the tower without CFRP plates strengthening, the initial stiffness of strengthened towers with CFRP plate prestresses of 0, 200, and 400 MPa increased by 71.0 %, 113.8 %, and 113.8 %, respectively. CFRP plate slacking occurred later for the strengthened tower with higher CFRP plate prestress. Moreover, when the specimens were in the same load, the displacement was significantly reduced for the specimen with CFRP plate prestress. The results showed that the prestressed CFRP plates strengthening method could improve the behavior of the system under wind load.

The final failure of specimen PS-400 is shown in Fig. 19. CFRP plate fracture and slacking occurred at tensile and compressive sides, respectively. The CFRP plate fracture was caused by the sharp support. Large transition arc at the end of the steel supports could be designed to ensure the safety of the CFRP plate. This was because maintaining a safe CFRP plate bending radius was crucial for ensuring the residual strength of the CFRP plate under flexural tensile loading [27]. Moreover, the slip between CFRP plate and anchorage at the tensile side occurred, resulting in a 27 mm displacement. The slip may be attributed to the insufficient bolt pretightening force or the uneven adhesive distribution. The stiffness of the prestressed strengthened steel tube decreased obviously after CFRP plate slacking at the compression side.

3.3.2. Availability of the strengthening method

For the prestressed CFRP plate strengthening method, the initial stiffness increased as much as 113.8 % when the CFRP plate prestress was 200 MPa. The results indicated that the prestressed CFRP plate strengthening method was effective for increasing the behavior of the tower under wind load. The application of equivalent concentrated load resulted in a stress distribution that was more unfavorable compared to wind pressure. Because the signal tower was safe under such a concentrated load, it could withstand the required wind pressure.

The stress state of different parts in the strengthening system was vital to the applicability of this method. For the column system, the maximum column strain at the tensile side of specimens PS-0, PS-200, and PS-400 under the load of 10, 10, and 19 kN was 286, 291, and 448 με, respectively, which were all far less than the yield strain of steel column (Fig. 20). It indicated that the column system was in a safe condition to anchor CFRP plates. For the support system, the maximum support strain at the tensile side of specimens PS-0, PS-200, and PS-400 under the load of 10, 10, and 19 kN was 89, 61, and 133 με (Fig. 21), respectively, and the buckling of steel support did not occur. It was safe for the support system. For anchorages, although some slippage occurred in the test due to the ununiform adhesive thickness, we could replace the self-designed anchorages with commercial ones when this strengthening method was applied in real engineering. For CFRP plates, the maximum CFRP plate stresses for specimens PS-0, PS-200, and PS-400 were 409, 604, and 1020 MPa (Fig. 22), respectively, and the CFRP plate ultimate strength is 2800 MPa. Although specimen PS-400 had CFRP fracture when CFRP plate stress was 1020 MPa, a larger transition arc at the end of the supports could be designed to achieve a larger bending radius of the CFRP plate and thus increase its security reserve [27].

4. Numerical analysis

4.1. Simulation procedure

The numerical studies were conducted by ABAQUS [23]. Solid element C3D8R and shell element S4R were used for steel and CFRP plates, respectively. The global mesh sizes for steel and CFRP plates were 10 mm and 5 mm, respectively (Fig. 23). 'Tie' constraint was used for the surface connection between different parts, i.e., the inner surfaces of hoops, and outer surface of tower; bottom surface of columns and upper surface of steel base; steel support surfaces and outer surface of hoops; steel support surfaces and column surfaces; CFRP surfaces and anchorage surfaces; CFRP plate surfaces and hoop surface; CFRP plate surfaces and steel support surfaces. The red area in Fig. 24 was the surface for the 'Tie' constraint. A reference point was set 50 mm above the center of the top steel tube and a 'coupling' constraint was used for the interaction between the point and the upper surface of the steel tube. The degrees of freedom of the steel base were all constrained to simulate a rigid boundary condition. The loading procedure of the static analysis was divided into two steps. In the initial step, CFRP plates were prestressed by setting the CTE of 1×10^{-5} and adjusting temperatures. Finally, the CFRP plate achieved a prestress of 400 MPa. In the second step, the displacement of 100 mm was applied to the reference point.

The densities of steel and CFRP plate are taken as 7185 and 1800 kg/m^3, respectively. The elastic modulus and yield strength of steel are 209 GPa and 499 MPa, respectively. The elastic modulus of the CFRP plate is 200 GPa. The Poisson's ratios of steel and CFRP plate are 0.3 and 0.2, respectively.

4.2. Verification

Specimen PS-400 was taken as an example for FEM verification, as shown in Figs. 25 and 26. Fig. 25 showed the load-displacement curve obtained by FEM and the experiment (EXP). The decrease in stiffness caused by CFRP plate slacking at the compressive side had the same tendency as the experiment. Fig. 26 (a) showed that the CFRP plate stress increase rate in the tension side of CFRP plate began to decrease after the stress was larger than 600 MPa. This was because the slip between the CFRP plate and anchorage occurred. The root mean square (RMS) error was used to assess the accuracy of the predicted values by FEM. The numerical and experimental load corresponding to every

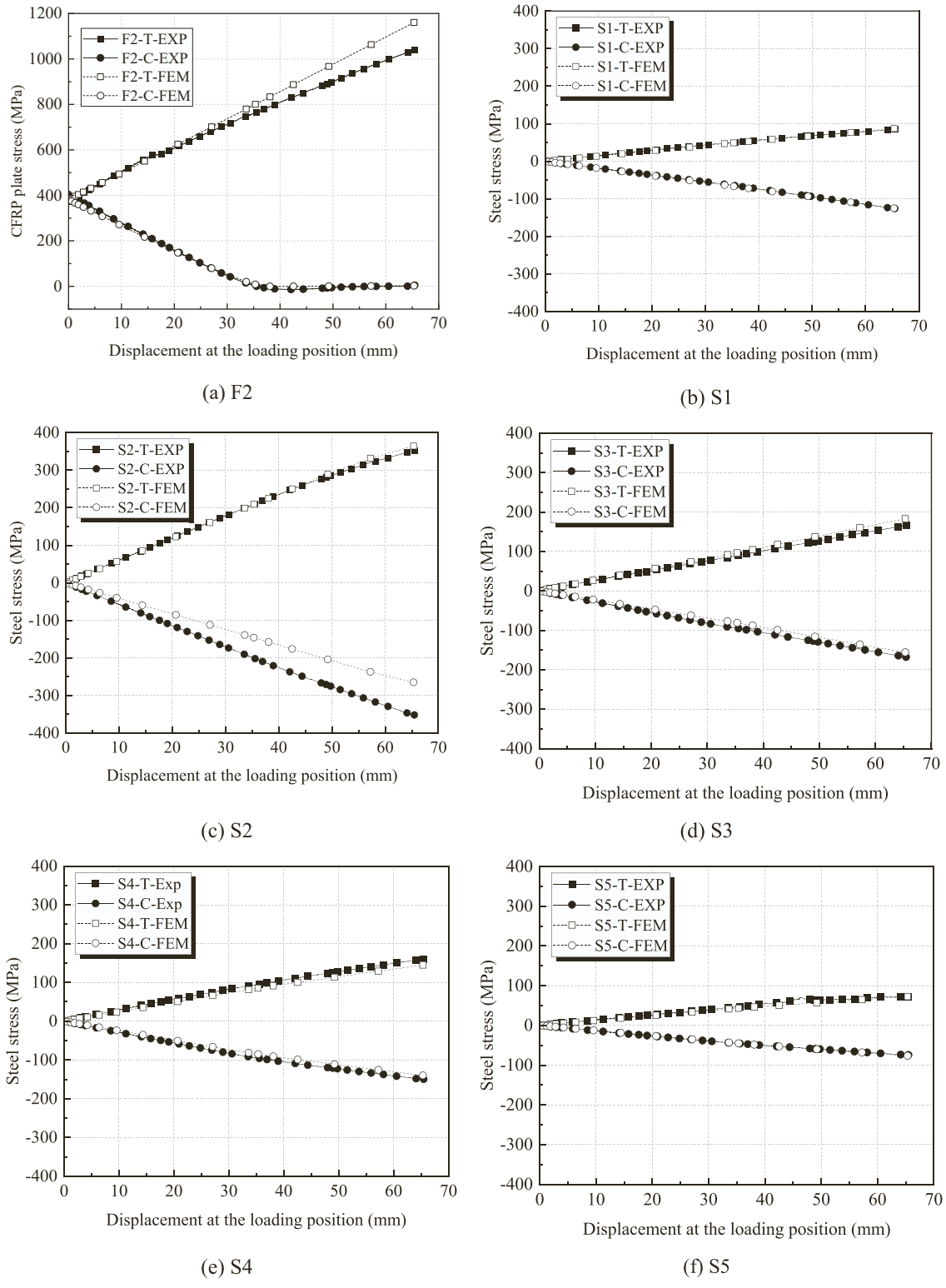


Fig. 26. Comparisons of CFRP plate stress-displacement curve at F2 and steel stress-displacement curve at S1–S5 between EXP and FEM.

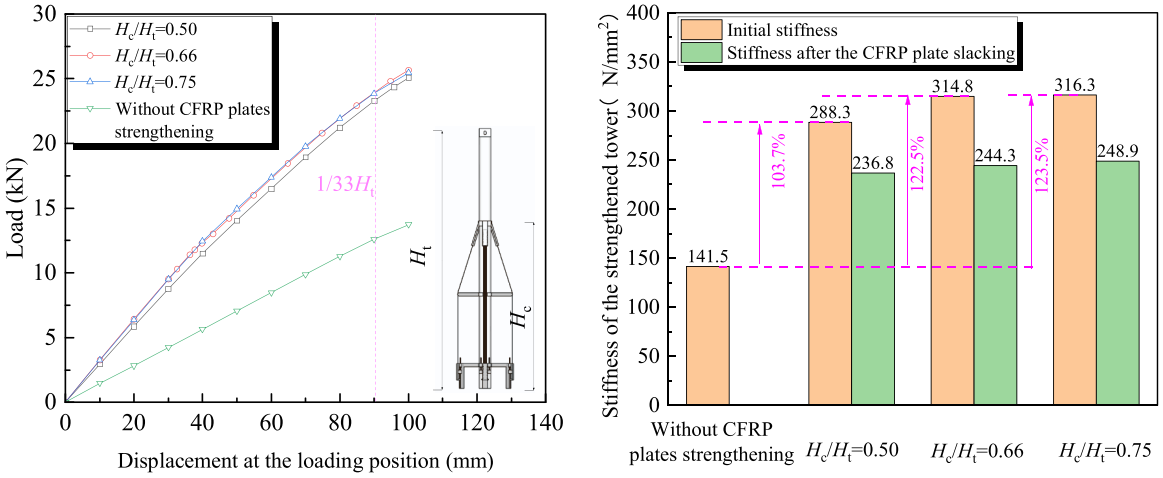
Table 4
Parametric analysis.

Model name	H_c/H_t	H_s/H_t	H_b/H_t	L_s/D_t	T_i/A_p (MPa)	E_p (GPa)
R1	0.66	0.38	0.1	1.82	400	200
R2	0.75	0.38	0.1	1.82	400	200
R3	0.50	0.38	0.1	1.82	400	200
R4	0.66	0.50	0.1	1.82	400	200
R5	0.66	0.20	0.1	1.82	400	200
R6	0.66	0.20	0.1	1.05	400	200
R7	0.66	0.20	0.1	1.35	400	200
R8	0.66	0.20	0.1	2.14	400	200
R9	0.66	0.38	0.1	1.82	0	200
R10	0.66	0.38	0.1	1.82	200	200
R11	0.66	0.38	0.1	1.82	800	200
R12	0.66	0.38	0.1	1.82	400	150
R13	0.66	0.38	0.1	1.82	400	250
R14	0.66	0.38	0.2	1.82	400	200
R15	0.66	0.38	0.3	1.82	400	200

10 mm were utilized for the RMS error calculation. The RMS errors for load, CFRP plate stress at F2, and steel stress at S1–S4 of specimen PS-400 were 0.55 kN, 3.18 MPa, 1.68 MPa, 4.31 MPa, 1.75 MPa, and 1.78 MPa, respectively, indicating satisfactory agreement between the numerical simulations and experiments. The slight difference of the steel strain at S2 between FEM and EXP may be attributed to the measurement in the test.

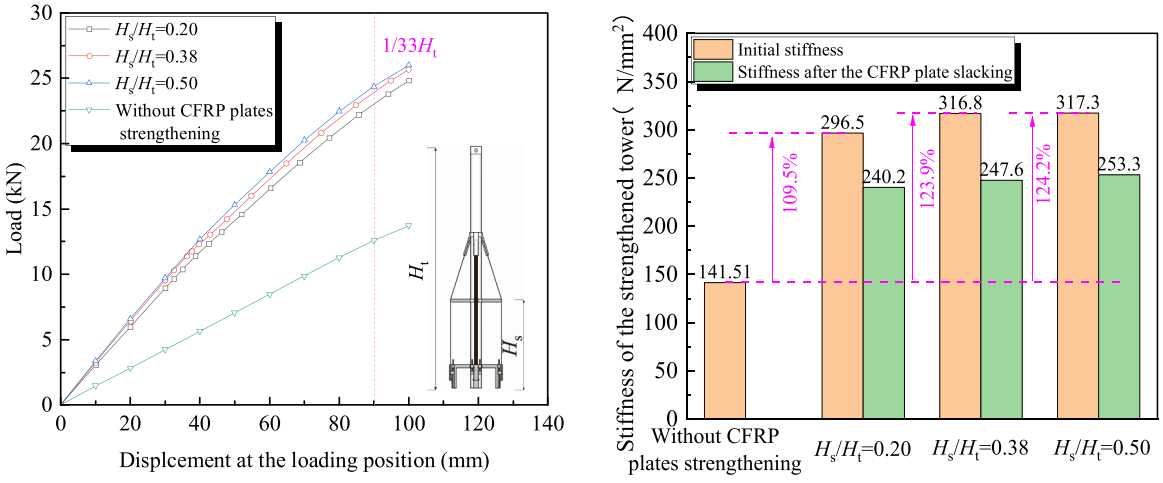
4.3. Parametrical study

As known from Section 2.1, the strengthening effect was influenced by H_c/H_t, H_s/H_t, H_b/H_t, L_s/D_t, T_i/A_p and E_p. Thus, the basic model was chosen as PS-400, and fifteen models were established in ABAQUS [23] to study the influence of the parameters (Table 4). H_s/H_t was taken as 0.5, 0.66 and 0.75; H_c/H_t was taken as 0.2, 0.38, and 0.5; H_b/H_t was taken as 0.1, 0.2, and 0.3 in the parametrical studies to study their effects. The value of L_s/D_t was determined by the CFRP plate bending angle. Specifically, bending angles of 10°, 13°, and 20° corresponded to the



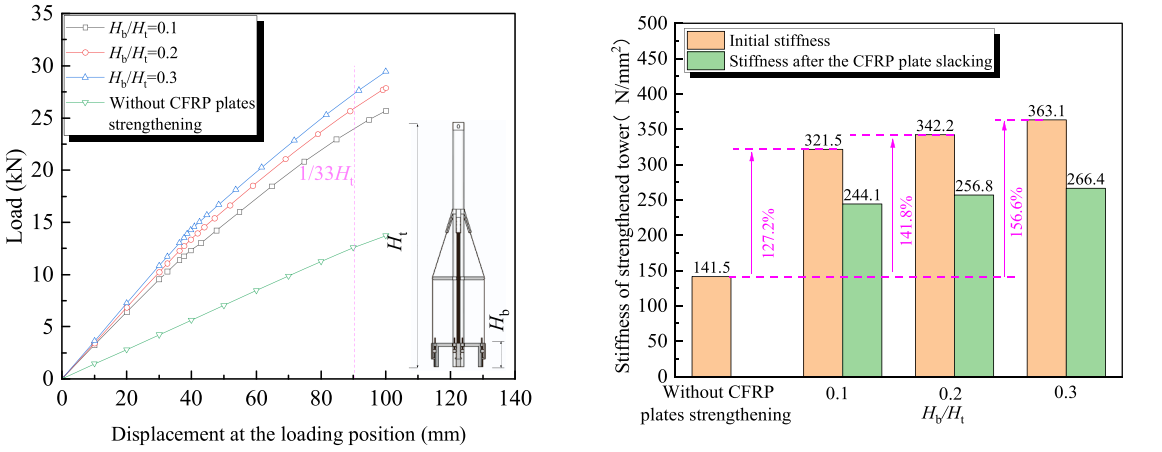
(a) displacement-load curve (b) stiffness before and after the CFRP plate slacking

Fig. 27. Load-displacement curve and stiffness of the strengthened tower with different H_c/H_t.



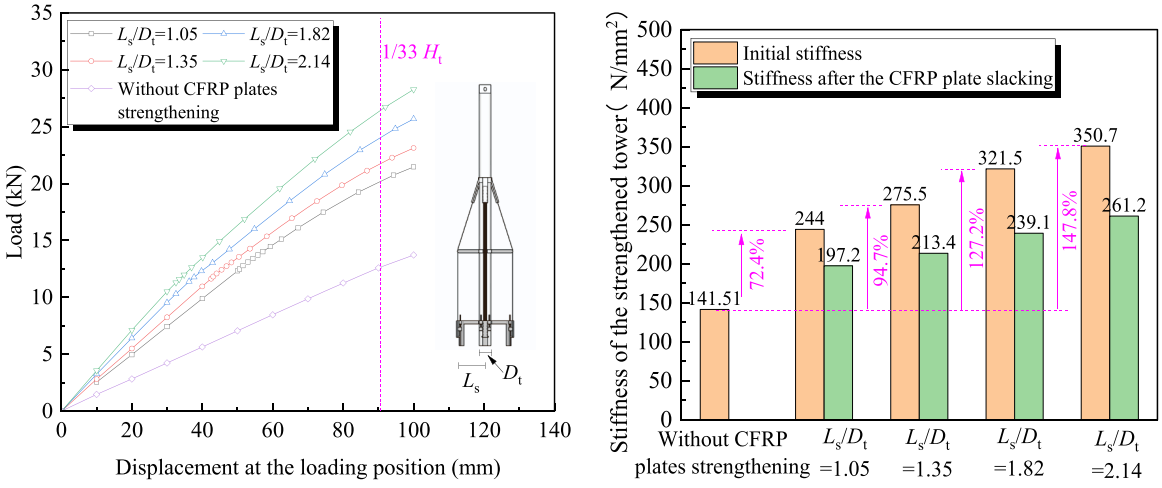
(a) displacement-load curve (b) stiffness before and after the CFRP plate slacking

Fig. 28. Load-displacement curve and stiffness of the strengthened tower with different H_s/H_t.



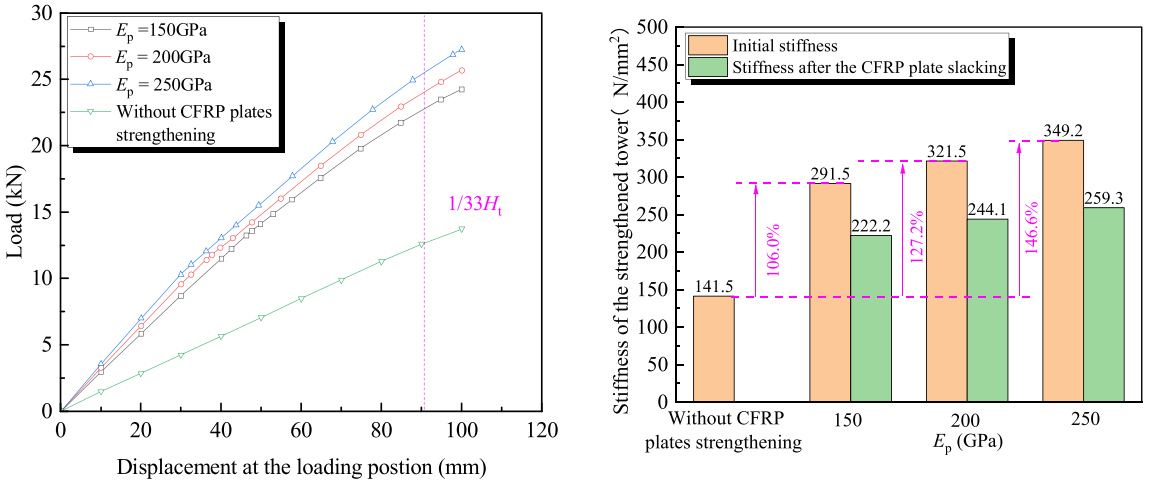
(a) displacement-load curve (b) stiffness before and after the CFRP plate slacking

Fig. 29. Load-displacement curve and stiffness of the strengthened tower with different H_b/H_t.



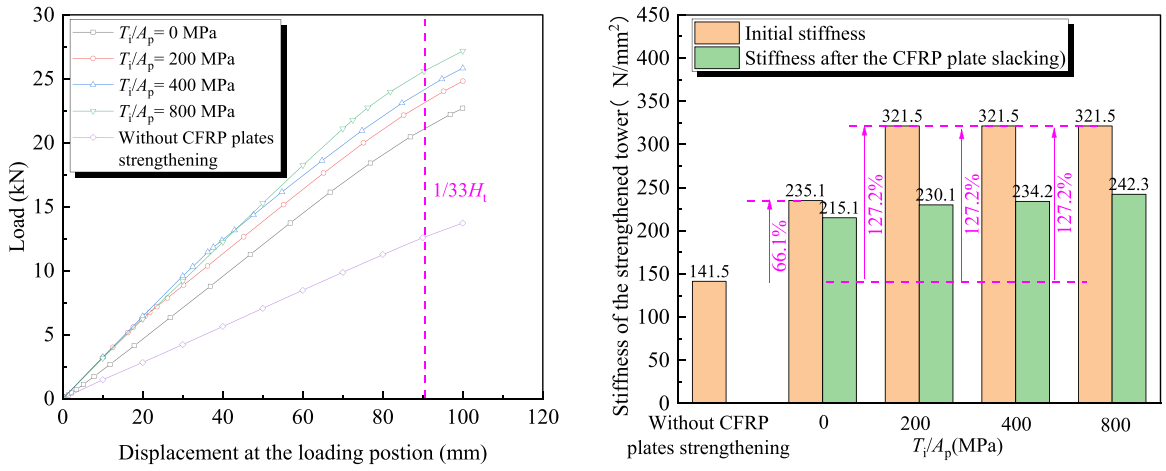
(a) displacement-load curve (b) stiffness before and after the CFRP plate slacking

Fig. 30. Load-displacement curve and stiffness of the strengthened tower with different L_s/D_t.



(a) displacement-load curve (b) stiffness before and after the CFRP plate slacking

Fig. 31. Load-displacement curve and stiffness of the strengthened tower with different E_p.



(a) displacement-load curve (b) stiffness before and after the CFRP plate slacking

Fig. 32. Load-displacement curve and stiffness of the strengthened tower with different T_i/A_p.

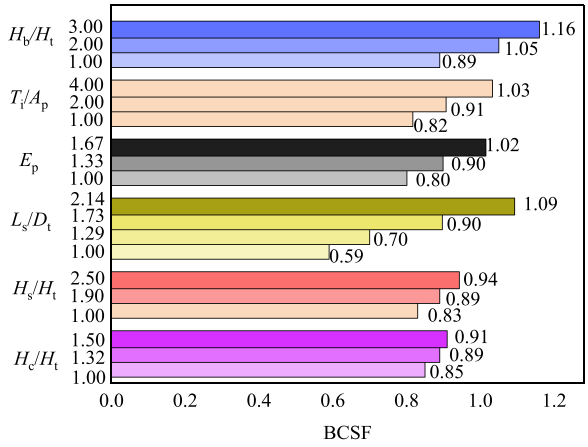


Fig. 33. BCSF of the strengthened tower with different parameters.

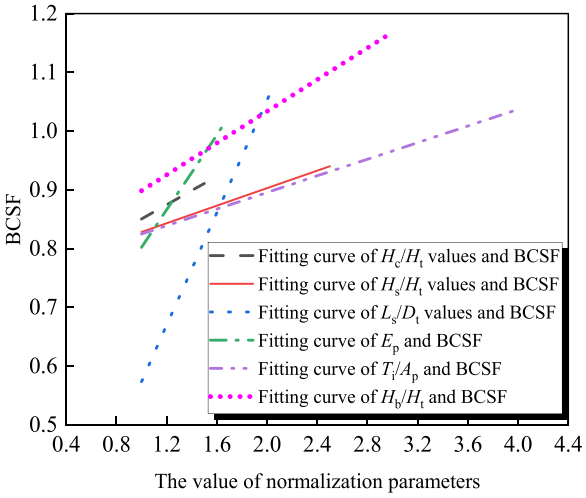


Fig. 34. The fitting curves of different parameter values and BCSF.

values of 1.05, 1.35, and 2.14 for L_s/D_t, respectively. The load corresponding to the ultimate displacement satisfying the standard requirement (1/33H_t) was defined as the bearing capacity.

4.3.1. *Effect of H_c/H_t*

The load-displacement curve and stiffness of strengthened tower with different H_c/H_t are shown in Fig. 27. When H_c/H_t increased from 0.50 to 0.66 and 0.75, compared with the unstrengthened tower, the bearing capacity increased by 85 %, 89 % and 91 %, respectively; the initial stiffness of the strengthened tower increased by 103.7 %, 122.5 %, and 123.5 % compared with the tower without CFRP plate strengthening (Fig. 27(a)), respectively; the ratios of stiffness after the CFRP plate slacking to the initial stiffness were 82.1 %, 77.5 %, and 78.7 %, respectively (Fig. 27(b)). It indicated that increasing H_c/H_t was beneficial to improve the behavior of the tower when H_c/H_t was small, however, the effect of the increase in H_c/H_t on improving the behavior was limited.

4.3.2. *Effect of H_s/H_t*

The load-displacement curve and stiffness of the strengthened tower with different H_s/H_t is shown in Fig. 28. When H_s/H_t increased from 0.28 to 0.38 and 0.66, compared with the unstrengthened tower, the bearing capacity increased by 82.7 %, 89.0 % and 94.3 %, respectively; the initial stiffness of the strengthened tower increased by 109.5 %, 123.9 %, and 124.2 % compared with the tower without CFRP plate strengthening (Fig. 28 (a)), respectively; the ratios of stiffness after the CFRP plate slacking to the initial stiffness were 81.0 %, 78.2 %, and 79.8 %, respectively (Fig. 28 (b)). It indicated that increasing H_s/H_t improved the stiffness of the strengthened tower and the bearing capacity of the tower, while the extent of the increase was limited.

4.3.3. *Effect of H_b/H_t*

The load-displacement curve and stiffness of the strengthened tower with different H_b/H_t is shown in Fig. 29. When H_b/H_t increased from 0.1 to 0.2 and 0.3, compared with the unstrengthened tower, the bearing capacity increased by 89.6 %, 104.8 % and 116.0 %, respectively; the initial stiffness of the strengthened tower increased by 127.2 %, 141.8 %, and 156.6 % compared with the tower without CFRP plate strengthening (Fig. 29 (a)), respectively; the ratios of stiffness after the CFRP plate slacking to the initial stiffness were 72.5 %, 81.5 %, and 88.3 %, respectively (Fig. 29 (b)). It indicated that increasing H_b/H_t significantly improved the stiffness and the bearing capacity of the tower.

4.3.4. *Effect of L_s/D_t*

The load-displacement curve and stiffness of strengthened tower with different L_s/D_t is shown in Fig. 30. When L_s/D_t increased from 1.05 to 1.35, 1.82, and 2.14, compared with the unstrengthened tower, the

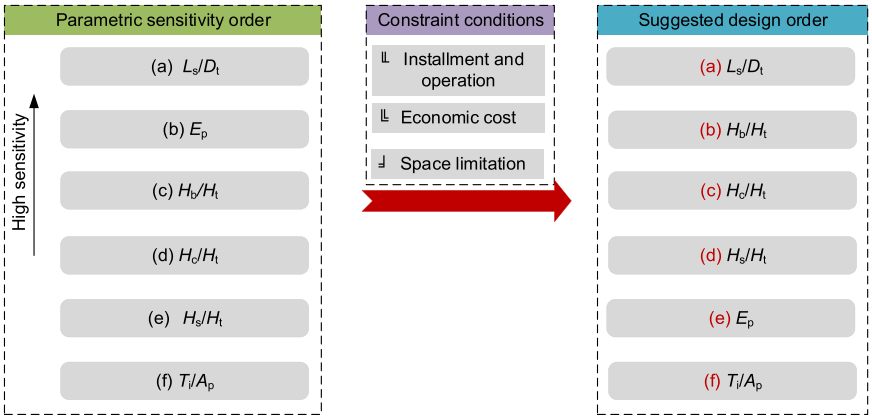


Fig. 35. Design order of the parameters.

bearing capacity increased by 59.0 %, 70.9 %, 89.7 %, and 109.3 %, respectively; the initial stiffness of strengthened increased by 72.4 %, 94.7 %, 127.2 %, and 224.1 %, respectively (Fig. 30 (a)); the ratios of stiffness after the CFRP plate slacking to the initial stiffness were 80.1 %, 77.3 %, 74.3 %, and 74.4 % respectively (Fig. 30 (b)). The results showed that increasing the steel support length significantly improved the behavior of the towers.

4.3.5. *Effect of T_i/A_p and E_p*

The load-displacement curve and stiffness of the strengthened tower with different T_i/A_p and E_p are shown in Figs. 31 and 32. When E_p increased from 150 to 200 and 250 GPa, compared with the unstrengthened tower, the bearing capacity increased by 80.1 %, 89.9 %, and 101.5 %, respectively; the initial stiffness of the strengthened tower increased by 106.0 %, 127.2 %, 146.6 % compared with the tower without CFRP plate strengthening, respectively (Fig. 31 (a)), the ratios of stiffness after the CFRP plate slacking to the initial stiffness were 62.0 %, 63.5 %, and 64.3 %, respectively (Fig. 31 (b)). The results indicated that increasing E_p improved the behavior of the tower under wind load.

When T_i/A_p increased from 0 to 200 MPa, the initial stiffness of strengthened towers increased significantly compared with the unstrengthened tower; while when T_i/A_p increased from 200 to 400 and 800 MPa, the initial stiffness of strengthened towers remained almost unchanged with the increase in T_i/A_p (Fig. 32 (a)). When T_i/A_p increased from 0 to 200, 400, and 800 MPa, the load corresponding to the ultimate displacement increased by 73.0 %, 81.7 %, 90.7 %, and 103.3 %, and the ratios of stiffness after the CFRP plate slacking to the initial stiffness were 91.4 %, 72.8 %, 72.9 %, and 75.3 %, respectively (Fig. 32 (b)). Moreover, the CFRP plate slacking occurred later for the strengthened tower with higher CFRP plate prestress. The results indicated that increasing CFRP plate prestress had a positive effect on increasing the initial stiffness of the tower, and there was a limit to further increase the initial stiffness when CFRP plate prestress reached a certain level; while the stiffness after the CFRP plate slacking kept increasing as T_i/A_p increasing.

4.4. *Recommendation of strengthening design procedure*

Parametric sensitivity was analyzed based on the results of Section 4.3 and the analysis method was as follows. First, the parameters were normalized. The bearing capacity strengthening factor (BCSF) was defined as the ratio of the bearing capacity of the strengthened tower to that of the unstrengthened tower. Then, BCSFs were compared for the strengthened tower with different H_c/H_t, H_s/H_t, H_b/H_t, L_s/D_t, E_p, and T_i/A_p (Fig. 33). Fig. 34 showed the fitting curves of different parameter values and BCSF. The parametric sensitivity was ranked as L_s/D_t, E_p, H_b/H_t, H_c/H_t, H_s/H_t, and T_i/A_p. For designing the strengthening system, the design orders of the parameters should not only consider the parametric sensitivity but also the constrained conditions, i.e., the difficulties in installation and operation, economic considerations, as well as space limitations, as shown in Fig. 35. First, because the sensitivity of L_s/D_t was the highest and L_s was limited by the surrounding space, the design of L_s/D_t should be considered first. Second, although the sensitivity of H_b/H_t, H_s/H_t and H_c/H_t was not as high as E_p, and the column height H_b influenced the prestressing device dimensions, H_s and H_c affected the complexity of the installment operation (e.g. the installment of the hoop (related to H_s) should avoid the pedal position), thus these parameters were designed following L_s/D_t. Third, although E_p exhibited a high sensitivity, because it could be easily adjusted by replacing the original CFRP plates, the consideration of this parameter in the design can be postponed. Moreover, the sensitivity of T_i/A_p was the lowest, and changing T_i/A_p was the most straightforward way to change the behavior of the strengthened tower, thus it can be considered after determining other parameters. Thus, the consideration sequence of these parameters in the design can be advanced. In sum, when the proposed strengthening method was applied, the design orders were determined as L_s/D_t, H_b/H_t, H_c/H_t, H_s/H_t, E_p, and T_i/A_p (Fig. 35).

5. Conclusion

The following conclusions can be obtained:

(1) A novel prestressed CFRP plate strengthening method for signal towers has been proposed, which has good advantages of significant strengthening effect, high installment efficiency, high-level prefabrication, and low strengthening and maintenance cost. The mechanism of prestressed CFRP plate strengthening methods was clarified. The strengthening elements synergistically interact with the tower and a self-balancing system was formed; thus, the stiffness of the tower increasd and the lateral displacement of the tower could be obviously reduced under wind load.

(2) Through experimental tests, the strengthening method can effectively improve the behavior of the system under wind load. Compared with the tower without strengthening, the initial stiffness of strengthened towers with CFRP plate prestresses of 0, 200, and 400 MPa increased by 71.0 %, 113.8 %, and 113.8 %, respectively; Moreover, the CFRP plate slacking occurred later for the strengthened tower with higher CFRP plate prestress and the stiffness of the tower after the CFRP plate slacking kept increasing as CFRP plate prestress increased.

(3) Finite element analysis was conducted to investigate the effect of parameters in the strengthening system on the behavior of strengthened towers. Increasing H_c/H_t, H_s/H_t, H_b/H_t, L_s/D_t, E_p, and T_i/A_p had a positive effect on improving the behavior of the strengthened tower under wind load. Finally, a strengthening

procedure was proposed to guide the design of the strengthening system, considering both the parametric sensitivity and the constraint conditions.

CRediT authorship contribution statement

Xu Liang: Writing – original draft, Software, Investigation, Formal analysis. **Yunhao Wang:** Writing – original draft, Validation, Software, Investigation. **Peng Feng:** Writing – review & editing, Methodology, Conceptualization. **Lili Hu:** Writing – review & editing, Writing – original draft, Supervision, Methodology, Funding acquisition, Conceptualization.

Declaration of Competing Interest

The authors declare that they have no known competing financial interests or personal relationships that could have appeared to influence the work reported in this paper.

Data availability

Data will be made available on request.

Acknowledgements

This research was supported by the Innovation Project of Beijing Jinmao Green Building Technology Co., Ltd., and Young Elite Scientists Sponsorship Program by CAST (2022QNRC001).

References

[1] Climate.gov. 2023: A historic year of U.S. billion-dollar weather and climate disasters. Available from: https://www.climate.gov/news-features/blogs/beyond-data/2023-historic-year-us-billion-dollar-weather-and-climate-disasters.
[2] Wan YD. Research on strengthening technology for communication tower. Steel Construction, 29; 2014. p. 14–7 (in Chinese) DOI:10.13206/j.gjg201408003.
[3] Wang S, Jia B, Tian JG. Research on reinforcement technology of existing communication steel tower. Sichuan Building Science, 45; 2019. p. 11–6 (in Chinese) DOI:10.19794/j.cnki.1008-1933.2019.01.003.
[4] Morrison Hershfield releases a tower reinforcement solution. Available from: https://www.rcrwireless.com/20021121/archived-articles/morrison-hershfield-releases-tower-reinforcement-solution-2.
[5] Hu JZ. A study on cover plate design and monopole strengthening application. Thin Walled Struct 2011:1098–107. https://doi.org/10.1016/j.tws.2011.04.002.
[6] Hutter Trankina simplified monopole tower reinforcing. Available from: http://www.htedesign.com/tower_reinforcing.htm.
[7] Liu QM. A non-invasive reinforcement solution of power transmission monopoles. Compos Struct 2021;259:113436. https://doi.org/10.1016/j.compstruct.2020.113436.
[8] Ferreira JG, Branco FA. Structural application of GRC in telesignal towers. Constr Build Mater 2007;21:19–28. https://doi.org/10.1016/j.conbuildmat.2005.08.003.
[9] Westower Dywidag monopole reinforcing system. Available from: https://westower.ca/.
[10] Wu ZB, Wu D. Talking about the seamless steel pipe reinforcement device of the tower body of the signal single-pipe tower. Constr Decor 2021:157–8.
[11] Fort Worth Tower, Inc. http://www.fwtinc.com/default.asp.
[12] Feng P, Hu LL, Zhao XL, Cheng L, Xu SH. Study on thermal effects on fatigue behavior of cracked steel plates strengthened by CFRP sheets. Thin-Walled Struct 2014;82(2)):311–20. https://doi.org/10.1016/j.tws.2014.04.015.
[13] Hu LL, Feng P, Zhao XL. Fatigue design of CFRP strengthened steel members. Thin Walled Struct 2017;119:482–98. https://doi.org/10.1016/j.tws.2017.06.029.
[14] Hu LL, Liang X, Feng P, Li HT. Temperature effect on buckling behavior of prestressed CFRP-reinforced steel columns. Thin Wall Struct 2023;188:110879. https://doi.org/10.1016/j.tws.2023.110879.
[15] Liang X, Wang WY, Hu LL, Feng P. Experimental and numerical study on high-temperature performance of prestressed CFRP-reinforced steel columns. Eng Struct 2024;301:117347. https://doi.org/10.1016/j.engstruct.2023.117347.
[16] Feng P, Hu LL. Steel columns strengthened/reinforced by prestressed CFRP strips: Concepts and behaviors under axial compressive loads. Compos Struct 2019;217:150–64. https://doi.org/10.1016/j.compstruct.2019.03.038.
[17] Hu LL, Feng P. Prestressed CFRP-reinforced steel columns under axial and eccentric compression. Compos Struct 2021;268:113940. https://doi.org/10.1016/j.compstruct.2021.113940.
[18] Guo B, Wang H, Shi LB. Application of basalt composite materials in the reinforcement of signal tower mast structure. Archit Eng Technol Des 2021:120–1.
[19] Lanier B, Schnerch D, Rizkalla S. Behavior of steel monopoles strengthened with high-modulus CFRP materials. Thin Walled Struct 2009;47:1037–47. https://doi.org/10.1016/j.tws.2008.10.010.
[20] AeroSolutions, LLC. AeroForce systems, monopole, and tower upgrades. Available from: http://www.aerosolutionsllc.com/index.html.
[21] Deng J, Fei ZY, Li JH, Li. Hang. Fatigue behaviour of notched steel beams strengthened by a self-prestressing SMA/CFRP composite. Eng Struct 2023;274:115077. https://doi.org/10.1016/j.engstruct.2022.115077.
[22] Deng J, Zhong MT, Li XD, Liu ZC, Li SX. Experimental study on improving the compressive property of damaged RC columns with prestressed SMA spirals. Eng Struct 2024;307:117916. https://doi.org/10.1016/j.engstruct.2024.117916.
[23] ABAQUS2021. Analysis of users' manual. Providence, RI, USA: Abaqus Inc.; 2021.
[24] YD/T5131–2019. Design specification of structure for mobile communication engineering steel tower and mast. Beijing, China: Ministry of industry and information technology of PRC; 2021.
[25] GB/T228.1–2010. Metallic materials-tensile testing-part l: method of test at room temperature. Beijing, China: China Standardization Administration; 2011. (in Chinese).
[26] GB50009–2019. Load code for the design of building structure. Beijing, China: Ministry of Housing and Urban-Rural Development of PRC 2018. (in Chinese).
[27] Xia J, Xu Z, Zhuge P, Wang B, Cai W, Fu J. Testing and evaluation of flexural tensile strength of prestressed CFRP cables. Materials 2022;15:7065.